A comparative study of the surface glaze characteristics of concrete treated with CO_2 and high power diode lasers Part I: Glaze characteristics

J. Lawrence* and L. Li

Manufacturing Division, Department of Mechanical Engineering, University of Manchester Institute of Science and Technology (UMIST), Manchester, M60 1QD, UK.

* Corresponding Author

Tel : (44) 161 236 3311 ext. 2383; fax : (44) 161 200 3803

E-mail address : j.lawrence@stud.umist.ac.uk

Abstract

This present work describes the differences in the characteristics of glazes generated on the ordinary Portland cement (OPC) surface of concrete by means of CO_2 and high power diode laser (HPDL) radiation. The value of such an investigation would be to facilitate the hitherto impossible task of generating a durable and long-lasting surface seal on the concrete, thereby extending the life and applications base of the concrete. The basic process phenomena are investigated and the laser effects in terms of glaze morphology, composition, phase and microstructure are presented. Also, the resultant heat affects are analysed and described. The glaze generated after HPDL interaction was found be fully amorphous in nature, whilst the glaze generated after CO_2 laser interaction was seen to be of a semi-amorphous structure, with sizeable areas, randomly located within the glaze, displayed a somewhat regular columnar structure. This is proposed to be due to the differing solidification rates occasioned by each laser after treatment as a result of differences in the beam absorption lengths.

Keywords: CO_2 laser; High power diode laser (HPDL); Concrete; Cement; Surface glazing; Microstructure; Solidification; Phase

1. Introduction

Lasers have unique characteristics that afford them the ability to be employed for the non-contact processing of materials which are otherwise difficult to process. One such material is concrete, which is a composite material consisting of an array of fine and coarse aggregate pieces embedded within a hardened ordinary Portland cement (OPC) paste. Consequently the processing and surface treatment of concrete can be an arduous task.

Much work has been carried out previously to investigate the laser processing of concrete. However, most of the research has concentrated on the laser cutting of concrete and reinforced concrete using high power CO_2 lasers, with a view, primarily, to nuclear reactor decommissioning [1-3]. Also, as part of nuclear plant decommissioning, Li et al. [4-7] conducted research to determine the workability of several laser techniques: direct glazing of the concrete, single and multiple layer fusion cladding and combined chemical/fusion cladding, for the sealing/fixing of radioactive contamination onto concrete surfaces. Further work by Johnston et al. [8] reported on the successful removal of the contaminated surface layer of concrete (scabbling) by means of Nd:YAG and CO_2 laser radiation. Work by Sugimoto et al. [9] focused upon modifying the surface appearance and surface properties of cement based materials using a high power CO_2 laser. The laser treatment produced novel surfaces, with surface textures, properties and appearance unique to laser treatment. The resultant physical characteristics and mechanical behaviour of the post-process cement based materials were later fully characterised by Wignarajah et al. [10]. Borodina et al. [11] have carried out investigations into the structural changes within the composition of zirconia concrete caused by surface exposure to CO_2 laser radiation, detailing microstructural changes, phase changes and the absorptivity characteristics.

In all of the previous studies conducted with CO_2 and Nd:YAG lasers, spallation and excessive cracking and pore formation were found to be major problems undermining the performance of the laser treated surface layer. In contrast, however, work conducted by Li et al. [12] and further work carried out by Lawrence et al. [13-15] using a high power diode laser (HPDL), successfully demonstrated the generation of a long-lasting glaze with far fewer cracks and pores.

To date, the comparative effects of CO_2 laser and HPDL radiation have not been reported Similarly, practical comparisons between the traditional materials processing lasers (CO_2, Nd:YAG and excimer lasers) and the more contemporary high power diode laser (HPDL) are limited. Previously, Schmidt et al. [16] compared the performance of CO_2, excimer and HPDL in the removal of chlorinated rubber

coatings from concrete surfaces, noting the existence of wavelength dependant differences in process performance. Bradley et al. [17] compared the CO_2 and HPDL for the treatment of Al_2O_3-based refractory materials in terms of microstructure. Work by Lawrence et al. concentrated on investigated the effects of CO_2, Nd:YAG excimer and HPDL on the wettability characteristics of engineering ceramics [18] an Al_2O_3/SiO_2-based ceramic [19] and a carbon steel [20]. In all the studies, the workers observed wavelength dependant microstructural characteristics unique to each laser.

This paper aims to elucidate the reasons behind the marked differences in the characteristics and performance of the glaze generated on the OPC surface of concrete when treated with CO_2 laser and HPDL radiation. Part I of the paper comparatively analyses the actual characteristics of the glazes, whilst in Part II the mechanical, physical and chemical properties of the glazes are compared.

2. Experimental procedures

The concrete studied in the experiments was the ubiquitous OPC based concrete. For the purpose of experimental convenience the as-received concrete blocks were sectioned into squares (120 mm x 120 mm x 20 mm) prior to laser treatment. The composition of the concrete by volume is as follows: 20mm limestone aggregate (40%), 10 mm limestone aggregate (14%), zone M sand (28.5%), OPC (10.5%) and particulate fine aggregate (7%).

The lasers used in this work were a CO_2 laser (RS1000, Rofin-Sinar) emitting at 10.6 μm with a maximum output power of 1 kW and a HPDL (D-60, Diomed) emitting at 810±20 nm with a maximum output power of 60 W. The CO_2 laser beam was delivered to the work surface by focusing the beam through a 125 mm focal length KC1 lens to give a stable diverging beam. The HPDL beam was delivered to the work area by means of a 4 m long, 600 μm core diameter optical fibre, the end of which was connected to a 2:1 focusing lens assembly. Both lasers were operated in the continuous wave (CW) mode and produced a multi-mode beam. The defocused laser beams were fired across the surface of the concrete samples by traversing the samples beneath the beams using the x- and y-axis of CNC gantry tables at speeds ranging from 60-600 mm min^{-1}. In both instances the laser optics were protected by means of a coaxially blown O_2 shield gas jet a rate of 5 l min^{-1}. In order to study accurately the differing effects of the two lasers, the power density of each was set at 2.25 kW cm^{-2}.

To determine the characteristics of the glazes the HPDL treated concrete samples were examined using optical microscopy, scanning electron microscopy (SEM), energy disperse X-ray analysis (EDX) and X-ray diffraction (XRD) techniques.

3. General effects of laser interaction with concrete

3.1 Depth of laser interaction and melting

It was found for both lasers that, as the traverse speed increased, the depth of the laser interaction area generally decreased (the depth of the laser interaction being the limit of the laser affected area visible under microscopic examination). Likewise, as the traverse speed increased, the depth of the laser melt region also generally decreased for both lasers. However, as is evident from Fig. 1, the depth of the laser interaction and melting observed differed somewhat between the two lasers. Regardless of the traverse speed, the laser interaction depth and the melt depth obtained after CO_2 laser glazing was consistently greater that that of the HPDL. More precisely, the melt depth obtained after CO_2 laser glazing was higher than that of the HPDL, whilst the laser interaction depth obtained after CO_2 laser glazing was considerably higher than that of the HPDL. Moreover, it can be seen clearly from Fig. 1 that the ratio of the laser interaction regions and the laser melt regions obtained with the CO_2 laser are much higher than those obtained with the HPDL. This indicates that the heat affected zone (HAZ) generated as a result of CO_2 laser treatment is much greater than that resulting from HPDL treatment.

3.2 Mass loss/regain during and after laser treatment

Although material ejection was generally not a typical feature of the glazing OPC surface of the concrete with either laser, a loss in mass of the concrete was a possibility due to the resulting heat effects of the process. In order to determine any weight loss experienced by the concrete as a result of laser irradiation, a number of samples were stored in a controlled environment for two days prior to laser irradiation. The samples were weighed regularly to ensure a constant mass. The samples were treated at various power densities and traverse speeds and then immediately weighed. Fig. 2 shows the percentage loss of original mass experienced by the concrete in terms of power density and traverse speed for both lasers

As one can see from Fig. 2, the loss in mass experienced by the concrete increases almost proportionately in a linear manner with increasing power density for both lasers, up to approximately 2.1 kW cm^{-2} for the HPDL and 1.8 kW cm^{-2} for the CO_2 laser. After this point the loss in mass can be seen to decrease in terms of the power density. It is reasonable to assume that this indicates that a level of power density saturation has been attained, beyond which further increases in power density have a marginal effect on the loss in mass of the concrete. In contrast, as the traverse speed is increased, then the loss in mass experienced by the concrete decreases for both lasers, again in a linear manner. It is clear from Fig. 2 that loss in mass experienced by the concrete is consistently higher when glazing with the CO_2 laser. This is perhaps not surprising when one considers that the HAZ generated as a result of CO_2 laser glazing is much larger than that generated when using the HPDL.

After laser treatment the samples were stored in an uncontrolled environment (open laboratory) and weighed regularly every day for 12 days. The results of these tests are given in Fig. 3, and show clearly that the extent to which the concrete regains mass is not only a function of the density of the energy deposited on its surface, but also of the laser used. This is perhaps to be expected for two reasons: firstly, an increase in the energy density increases the likelihood of material ejection or pore formation; and secondly, as Fig. 2 showed, the mass loss experienced by the concrete was consistently higher when exposed to CO_2 laser radiation, therefore reducing the amount of possible mass regain.

The general mass regain experienced by the laser treated concrete at the various laser power densities is thought to be the result of the rehydration through contact with the air of the HAZ, which is comprised of unslaked lime (as discussed later). This appears to be a reasonable assumption when one considers that in terms of absolute mass regain, the greatest mass regain was observed to occur with the samples treated with the highest power density.

4. Morphological and microstructural analysis

The typical surface morphology of the glazes generated on the OPC surface of the concrete when using (a) the CO_2 and (b) the HPDL are shown in Fig. 4. As is evident from Fig. 4, crack and pore formation was a common feature of both laser glazes. However, cracking and more prominently, pore formation occurred less on the HPDL generated glaze. The fracture sections of the glazes generated

on the OPC surface of the concrete when using (a) the CO_2 and (b) the HPDL are shown in Fig. 5, with the differences in the glaze microstructures being clearly visible.

Although the majority of the CO_2 laser induced glaze appeared to be of an amorphous structure, sizeable areas, randomly located within the glaze, displayed the somewhat regular columnar structure shown in Fig 5(a). In contrast, as one can see from Fig. 5(b), the microstructure of the HPDL generated glaze has no discernible structure and appears to be fully amorphous. Indeed, these findings were further confirmed by an XRD analysis of both the CO_2 and the HPDL generated glazes (Fig. 6), which revealed the HPDL induced glaze to be fully amorphous, whilst the CO_2 laser induced glaze was found to posses some crystallinity. From Fig. 6(b) it can be seen that traces of SiO_2 were not detected, whilst the Al_2O_3 appeared to be depleted. Yet, an EDX analysis revealed that the Si and Al were still present in similar proportions on the OPC surface before and after laser treatment. This is perhaps an indication that the OPC surface incident with the CO_2 laser has undergone partial vitrification due to the fact that these materials are glass forming elements, and consequently, vitrified when irradiated. Additionally, it is important to note that the peaks in Fig. 6(a) which are unmarked, for ease of analysis since they are not of direct interest, are likely to be tobermorite ($Ca_5(Si_6O_{18}H_2)4H_2O$) which provides diffraction peaks in the range 40 to 55^0, and rosenhahnite ($Ca_3SiO_3O_9H_2O$) which provides diffraction peaks in the range 40 to 70^0. Further, the peaks in Fig. 6(b) which have been left unmarked for the same reason, are likely to be mullite ($Al_6Si_2O_{13}$) which provides diffraction peaks in the range 35 to 40^0, scawtute ($Ca_6Si_6O_{18}2H_2O$) which provides diffraction peaks in the range 25 to 45^0, and quartz (low SiO_2) which provides diffraction peaks in the range 25 to 60^0. Also, some formation of spinel ($MgAl_2O_4$) would perhaps be expected; this, however, was not detected.

The columnar structure observed in the CO_2 laser generated glaze is similar to those previously reported by other workers who have treated Al_2O_3-based ceramics with CO_2 lasers. Lee and Gahr [21] and Bradley et al. [17] concluded that the columnar grains were comprised mainly of α- Al_2O_3. After CO_2 laser treatment of an Al_2O_3-based plasma-sprayed coating, Shieh and Wu [22] observed a similar columnar structure to that shown in Fig. 5(b), but with a zone of equiaxed grains on top of a columnar structure. Such a finding implies that there are two solidification fronts: one from the melt/substrate interface and another from the melt/air interface. Thus, if the two fronts meet solidification is complete. When the melt depth is shallow, the conductive heat loss is so fast that surface

solidification has insufficient time to develop. In contrast, when the melt depth is great, surface solidification occurs before the zone reaches the surface.

5. Heat affected zone analysis

Petzold et al. [23] have determined from differential thermal analysis (DTA) results that up to approximately 420^0C, concrete remains relatively stable. Notwithstanding this, some dehydration does occur and water is also lost from the pores of the cement. This is, however, far outweighed by the dehydration of $Ca(OH)_2$ which follows shortly after 420^0C is exceeded in accordance with

$$Ca(OH)_2 \rightarrow CaO+H_2O \qquad (1)$$

Furthermore, the dehydration of the $Ca(OH)_2$ promotes the development of microcracks which begin initially around the $Ca(OH)_2$ [24]. Moreover, this dehydration results in unslaked lime (CaO), which is effectively the generated HAZ; since the temperature of the surface of the concrete during interaction with both lasers during glazing was measured to be well in excess of 420^0C. This generated CaO HAZ was observed located either below the glazed surface layer or around the edges of the glazes. Indeed, by using a phenolphthalein indicator followed by water misting, it was possible to clearly discern the HAZ around the laser treated zone on the OPC surface of the concrete, since phenolphthalein is an indicator which is colourless in CaO, turning violet-red in the presence of $Ca(OH)_2$ due to the change in pH.

6. Discussion

6.1 Glaze formation mechanisms

The chemistry of the OPC surface of concrete and the hydration of its various constituents is extremely complex, and as such is not yet fully resolved [25]. Nevertheless, it is known that the constituents of OPC are minerals which exist as multi-component solid solution chemical compounds. One of the major constituents of OPC is Ca, however, of particular importance with regards this study, OPC contains in relatively large proportions: SiO_2 (21wt%), Al_2O_3 (5wt%) and Fe_2O_3 (3wt%), which are basic glass network formers and modifiers. Consequently the intense local heating brought about by the incident CO_2 and HPDL beams results in the melting of these

compounds at around 1283^0C, thereby causing the materials to lose the retained water and form an amorphous glassy material consisting of various calcium-silicate-alumina compounds [4]. Indeed, the semi- and fully amorphous nature of the CO_2 and HPDL generated glazes respectively was verified by an XRD analysis.

As was mentioned earlier, both CO_2 and HPDL interaction with the OPC surface occasioned a dramatic colour change; changing from grey to green. Such a change can be ascribed to the resultant phase transitions, and also the presence in small concentrations of metal transition ions in various oxidation states within the OPC composition, in particular, ferric ions in the Fe^{3+} and Fe^{2+} oxidation state. Fe^{3+} and Fe^{2+} ions are known to give rise to green and blue colours respectively when subjected to intense heating [25, 26]. However, if both phases are present within the composition, then the colour is determined by the Fe^{3+}/Fe^{2+} ion ratio, resulting in dark blue or black colours [25, 26]. Since the surface produced after CO_2 and HPDL treatment was green, then it is reasonable to assume that both phases were not present within the OPC.

6.2 Cracking and pore formation

As Fig. 4 shows, cracking of the CO_2 and HPDL induced glazes occurred to various degrees depending upon the laser used. The formation of cracks can be attributed mainly to thermal stresses generated during laser irradiation. This is due to the fact that OPC has low thermal conductivity, and, as such, during laser heating a large thermal gradient between the melt zone and the substrate exists which results in the generation of thermal stresses. Additionally, despite the fact that the laser surface treatment process is effectively localised in nature, the fact remains that a certain amount of the heat generated will be conducted to sections of the OPC where the surface is already glazed. This, combined with existence of a relatively cold OPC substrate means that thermal stresses will be generated. During the heating phase the stresses will be compressive and relieved by plastic deformation, thus precluding crack formation. At high temperatures ($T \geq T_m$) the stresses can also be relieved [27-29]. However, during cooling when the temperature falls below T_m, then stresses will accumulate. If the fracture strength of the material is exceeded, then cracking within the melted layer will occur. The thermal stress σ, induced by a thermal gradient can be calculated using the Kingery equation:

$$\sigma = \frac{E\alpha\Delta T}{1-\upsilon} \qquad (2)$$

where E is Young's modulus, ΔT is the temperature change, α is the coefficient of thermal expansion and ν is Poisson's ratio. More succinctly, ΔT is the difference between the critical temperature (below which stresses can no longer be relieved) and ambient temperature. For OPC this is the difference between the melting point, 1283^0C and ambient temperature 20^0C. So, if it is assumed that the glass formed on the surface of the OPC is similar to soda-lime-silica glass because the compositions of the two materials are similar, then by using the following values for a typical soda-lime-silica glass: E=6.42 x 10^4 MN m^{-2}, α=33 x 10^{-7} K^{-1}, ΔT=1263^0C and ν=0.176, when the OPC surface of the concrete was irradiated by the HPDL beam the thermal stress produced in the resulting glass according to Equation (2) was around 305 MN m^{-2}. Since this is well in excess of the fracture strength of the glass, 120 MN m^{-2} [30], cracking will occur, and can only be avoided by severe distortion or through the reduction of ΔT by pre-heating.

From Fig. 4 it can be seen that pores were a common feature of the CO_2 and HPDL induced glazes, varying in size from microscopic pits to large craters depending upon both the laser operating parameters and the actual laser employed. For all instances of pore formation the mechanism behind their development is the consequence of gas escaping from within the melt and disrupting the surface [31]. With regard to the OPC glaze, the gas is likely to be CO_2 [10]. If the laser energy density incident on the OPC is too low, then the generated CO_2 can not escape from the molten OPC surface easily because of the high viscosity of the melt. As such, when the CO_2 gas eventually does penetrate the melt surface, the resultant pore is not filled by the flow of the melt; since the insufficient energy density is unable to maintain a high enough temperature for an adequate length of time and thus decrease the overall viscosity of the melt [32]. In this case the pores formed are typically small and shallow, being regular in both periodicity and intensity . On the other hand, if the laser energy density incident on the OPC surface of the concrete is too high, then boiling of the surface may happen. At the same time an increase in CO_2 gas formation may occur within the melt. These individual pockets of CO_2 gas formation may combine and rise to surface of the melt. Once the energy density decreases (as the laser traverses away), then the additional CO_2 gas will attempt to escape from the molten surface. However, the solidifying melt will prevent this, causing bubbles to form. The excessive CO_2 gas pressure will firstly cause the bubbles to expand and ultimately rupture the walls of the bubbles creating a sharp 'knife edge' pore [3, 10]. These types of pore are usually large, deep and randomly spaced.

6.3 Differences in morphological and microstructural characteristics

As one can see from Fig. 4, the morphological characteristics of both the CO_2 and HPDL generated glazes were somewhat similar in appearance, albeit that the CO_2 laser generated glaze displayed more microcracks and pores. On the other hand, however, the microstructural characteristics of the glazes were quite different in nature.

Although the CO_2 laser generated glaze was for the most part amorphous, sizeable crystalline areas, randomly located, displaying a regular columnar structure were nevertheless observed. In contrast, the HPDL glaze was found to be fully amorphous in nature. It is well established that microstructural characteristics are determined by solidification rate [33-35]. Since the laser operating parameters used were identical, the marked microstructural differences observed between the CO_2 and the HPDL induced OPC glazes can therefore be attributed to the differing rates of solidification occasioned by the two lasers. Clearly, such differences in the solidification rates induced by each laser must be the result of differences in the actual beam characteristics of each laser and the effects thereof on the beam interaction characteristics with the OPC surface. Work carried out by Lawrence and Li [36], to investigate the absorption length of CO_2 and HPDL beams in the OPC surface of concrete, revealed that CO_2 laser radiation was absorbed to a significantly greater depth by the OPC than HPDL radiation. Thus, the melting of the OPC to greater depth is consequently effected after CO_2 laser interaction. This in turn produces differing solidification conditions within the CO_2 and HPDL generated melt pools. It is proposed that, under the selected laser operating parameters, the solidification rate resulting from CO_2 laser interaction was not sufficiently high to produce a fully amorphous glaze, yielding instead a partially crystalline structure. On the other hand, it is believed that the solidification rate resulting from HPDL interaction was sufficiently high to cause the complete vitrification of the OPC surface. Evidence of the validity of such postulations was in some way confirmed in experiments where the CO_2 laser energy density incident on the OPC surface was increased (2.25 kW cm^{-2} power density and 240 mm min^{-1} traverse speed). Whereas previously only semi-amorphous glazes were possible, the energy density levels were such that it was possible to generate fully amorphous glazes. However, the energy densities required were so high, that the glazes generated were extremely poor, with many microcracks and pores which thus rendered the glazes impractical. Furthermore, this increase in the dimensions of the melt pool resulting from CO_2 laser interaction could arguably be ascribed as the cause of the observed increase in the HAZ generated after CO_2 laser glazing; since the larger melt pool will inherently generate more heat.

6.4 Stability to devitrification

Despite the fact that interaction of the HPDL with the OPC surface of the concrete generated an amorphous glaze, it is a distinct possibility that the OPC glaze could become crystalline through the destruction of the glassy state by means of a process known as devitrification. This can occur as either the breakdown of the glass surface by corrosion or weathering, or as a result of the overall composition remaining unchanged while the crystals separate in the glassy medium, therefore destroying the glassy state. This process being entirely dependant upon the temperature and composition of the glass.

A high magnification SEM examination of the OPC glaze generated by the HPDL interaction revealed no evidence of devitrification within the OPC glaze. This indicates that exposure of the OPC glaze to the extremely harsh reagents detailed in Part II of this paper did not cause the glazes to devitrify. Nor did the glass devitrify as a result of favourable high temperatures and glass composition. This is of great significance since devitrification in this manner is the result of the movement of atoms to allow orientation and the presence of crystallisation centres. Such centres occur usually at the glass/air boundary, around a pore [37]. Clearly, as Fig. 1 and Fig. 2 show, pores were in general a common feature of the OPC glaze, particularly the CO_2 laser generated glaze. Furthermore, it is highly likely that the composition of the OPC glaze also played an important part in the stability to devitrification of the glaze. In particular it is known that compounds such as Al_2O_3 and MgO (which an EDX analysis showed were readily present in the OPC glazes) are known to be very useful in assuaging devitrification problems [37]. This is because the inclusion of such compounds within the OPC glaze composition creates an glaze without a high liquidus temperature and therefore a reduced tendency towards devitrification [37].

7. Conclusions

Using a 1 kW CO_2 laser and a 60 W-cw high power diode laser (HPDL), glazing of the ordinary Portland cement (OPC) surface of concrete was successfully demonstrated. Under the selected laser operating parameters (which gave the optimum quality glazes for both lasers), similarities and clearly discernible differences in the characteristics of the glazes generated by each laser were observed.

In both cases the dehydration of $Ca(OH)_2$ in the hardened cement paste was ascertained as forming the heat affected zone (HAZ). Cracks and pores were common features of the laser glazes. Cracking

was identified as being due to the generation of thermal stresses in excess of the fracture strength of the glazes. Pores are believed to be the result of CO_2 formation which ruptures the molten surface as it forms bubbles in an attempt to escape into the atmosphere.

The depth of melting resulting from CO_2 laser glazing, along with the depth of the HAZ, were found to be greater than those obtained with the HPDL. It is asserted that these differences in depths, in particular the HAZ depths, were responsible for the greater loss in mass after CO_2 laser glazing, and the greater mass regain after HPDL glazing, experience by the OPC. This is believed to be caused by the differences that exist between the CO_2 and HPDL beam absorption characteristics of the OPC. Moreover, the glaze generated after HPDL interaction was found be fully amorphous in nature, whilst the glaze generated after CO_2 laser interaction was seen to be of a semi-amorphous structure, with sizeable areas, randomly located within the glaze, displayed a somewhat regular columnar structure. Again, it is proposed that these microstructural difference are the result of the differing absorption characteristics effecting different solidification rates within the laser generated melt pools.

The mechanical testing and an analysis of the corrosion properties of the OPC glazes, as well as their life characteristics, are presented in Part II of this paper.

References

1. K. Sugita, M. Mori, T. Fujioka, Concrete Eng. 24 (1986) 13-22.
2. M. Hamasaki, Proceedings of The International Symposium on Laser Processing, San Jose, May 1987, pp. 158-167.
3. H. Yoshizawa, S. Wignarajah, H. Saito, Trans. Japan Welding Soc. 20 (1989) 31-36.
4. L. Li, P.J. Modern, W.M. Steen, Proceedings of LAMP '92: Science and Applications, Nagaoka, June 1992, (High Temperature Society of Japan, Osaka, 1993), pp. 843-848.
5. L. Li, W.M. Steen, P.J. Modern, Proceedings of ISLOE '93, Singapore, November 1993, (National University of Singapore, Singapore, 1994), pp. 25-30.
6. L. Li, W.M. Steen, P.J. Modern, J.T. Spencer, Proceedings of RECOD '94, London, April 1994, (SPIE, Bellingham, 1994), pp. 24-28.
7. L. Li, W.M. Steen, P.J. Modern, J.T. Spencer, Proceedings of EUROPTO '94: Laser Materials Processing and Machining, Frankfurt, June 1994, (SPIE, Bellingham, WA, 1994), pp. 84-95.
8. E.P. Johnston, G. Shannon, W.M. Steen, D.R. Jones, J.T. Spencer, Proceedings of ICALEO '98: Laser Materials Processing, November 1998, Orlando, Vol 85E, (Laser Institute of America, Orlando, 1999), pp. 210-218.
9. K. Sugimoto, S. Wignarajah, K. Nagasi, S. Yasu, Proceedings of ICALEO '90: Laser Materials Processing, Boston, November 1990 , (Laser Institute of America, Orlando, 1991), pp. 302-312.
10. S. Wignarajah, K. Sugimoto, K. Nagai, Proceedings of ICALEO '92: Laser Materials Processing, Orlando, October 1992, (Laser Institute of America, Orlando, 1993), pp. 383-393.
11. T.I. Borodina, G.E. Valyano, N.I. Ibragimov, E.P. Pakhomov, A.I. Romanov, L.G. Smirnova, P.K. Khabibulaev, J. Phys. and Chem. of Mater. Treatment 25 (1995) 541-546.
12. L. Li, J. Lawrence, J.T. Spencer, Proceedings of SPIE: Europto'97 Lasers in Material Processing, Munich, June 1997, Vol 3097, (SPIE, Bellingham, WA, 1997), pp. 600-611.
13. J. Lawrence, L. Li, Proceedings of ICALEO '99: Laser Materials Processing, San Diego, CA, November 1999, Vol 86D, (Laser Institute of America, Orlando, 1993), pp. 334-353.
14. J. Lawrence, L. Li, J. of Laser Applications. Accepted for publication.

15. J. Lawrence, L. Li, J. of Laser Apps. Accepted for publication.

16. M.J.J. Schmidt, L. Li, J.T. Spencer, App. Surf. Sci. 138-139 (1998) 378-384.

17. L. Bradley, L. Li, F.H. Stott, App. Surf. Sci. 138-139 (1998) 522-528.

18. J. Lawrence, PhD Thesis, UMIST, 1999.

19. J. Lawrence, L. Li, J. of Phys. D 32 (1999) 1075-1082.

20. J. Lawrence, L. Li, J. of Phys. D 32 (1999) 2311-2318.

21. S.Z. Lee, K.H. Gahr, Mat. Wiss. und Wekstofftech. 23 (1992) 117-123.

22. J.H. Shieh, S.T. Wu, App. Phys. Lett. 59 (1991) 1512-1514.

23. A. Petzold, M. Rohrs, Concrete for High Temperatures, MacLaren & Sons, London, 1970, pp. 40-85.

24. U. Schneider, U. Diederichs, Betonwerk & Fertigteil - Technik 3 (1981) 141-149.

25. G.D. Taylor, Construction Materials, Longman Scientific & Technical, London, 1991, pp. 31-34.

26. N. Jackson, R.K. Dhir, Civil Engineering Materials, MacMillan Press, New York, 1992, pp. 90-92.

27. F.S. Galasso, R. Veltri, Ceramics Bull. 62 (1983) 253-255.

28. R. Sivakumer, B.L. Mordike, J. Surf. Eng. 4 (1988) 127-140.

29. J. Mazumder, Optical Eng. 30 (1991) 1208-1219.

30. R.H. Doremus, Glass Science, John Wiley & Sons, New York, 1994, pp. 154-160.

31. M.H. Lewis, Glasses and Glass-Ceramics, Chapman & Hall, London, 1989, pp. 88-95.

32. Z. Lui, PhD Thesis, University of Liverpool, 1991.

33. O. Esquivel, J. Mazumder, M. Bass, S.M. Copely, in: R. Mehrabian, B.H. Kear & M. Cohen (Eds.), Rapid Solidification Processing, Principles and Technologies II, Claitors Publishing, Baton Rouge, LA., USA, 1980, pp. 150-173.

34. R.L. Ashbrook, Rapid Solidification Technology: Source Book, ASM International, Metals Park, 1983.

35. R. Mehrabian, Int. Metals Reviews 27 (1982) 185-209.

36. J. Lawrence, L. Li, J. of Phys. D, submitted.

37. J.H. Dickson, Glass: A Handbook for Students and Technicians, Hutchinsons Scientific and Technical Publications, London, 1951, pp. 108-111.

List of Figures

Fig. 1

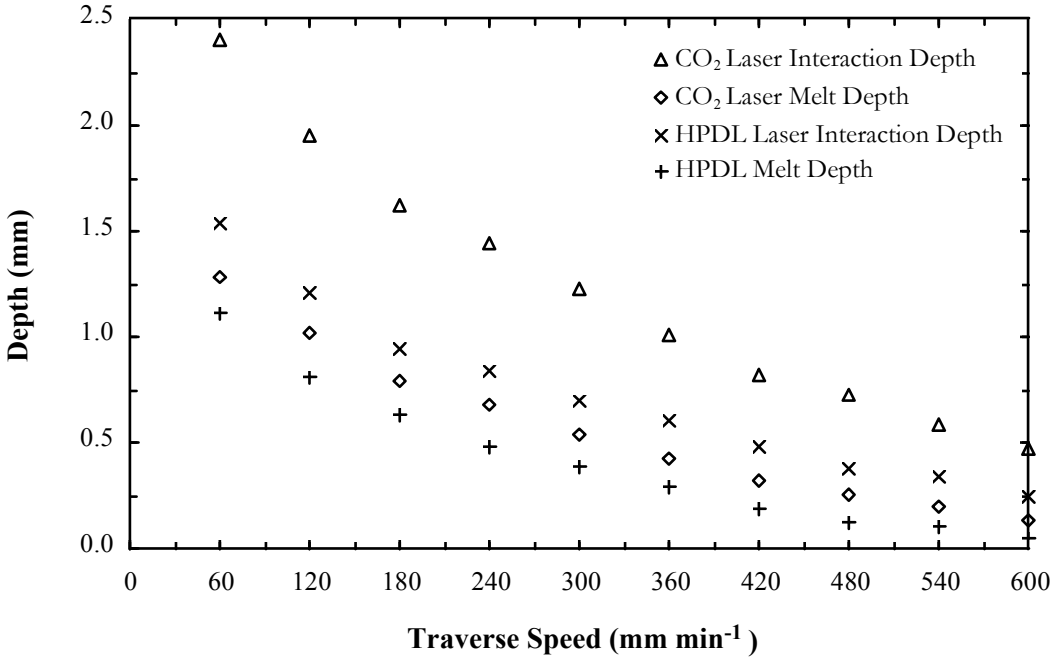
2.5
2.0
1.5
1.0
0.5
0.0
Depth (mm)
0
60
120
180
240
300
360
420
480
540
600
Traverse Speed (mm min-1)
CO2 Laser Interaction Depth
CO2 Laser Melt Depth
HPDL Laser Interaction Depth
HPDL Melt Depth

Fig. 2

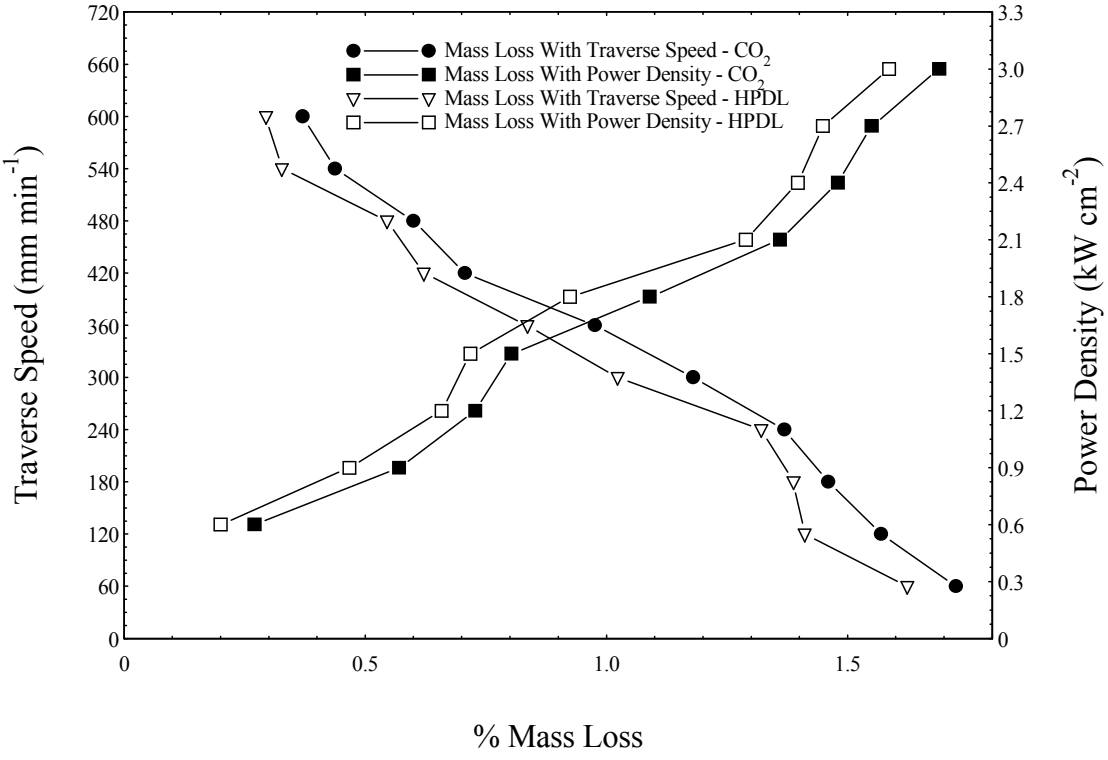
Mass Loss With Traverse Speed - CO_2
Mass Loss With Power Density - CO_2
Mass Loss With Traverse Speed - HPDL
Mass Loss With Power Density - HPDL
Traverse Speed (mm min^{-1})
Power Density (kW cm^{-2})
% Mass Loss
0
60
120
180
240
300
360
420
480
540
600
660
720
0.3
0.6
0.9
1.2
1.5
1.8
2.1
2.4
2.7
3.0
3.3
0.5
1.0
1.5

Fig. 3

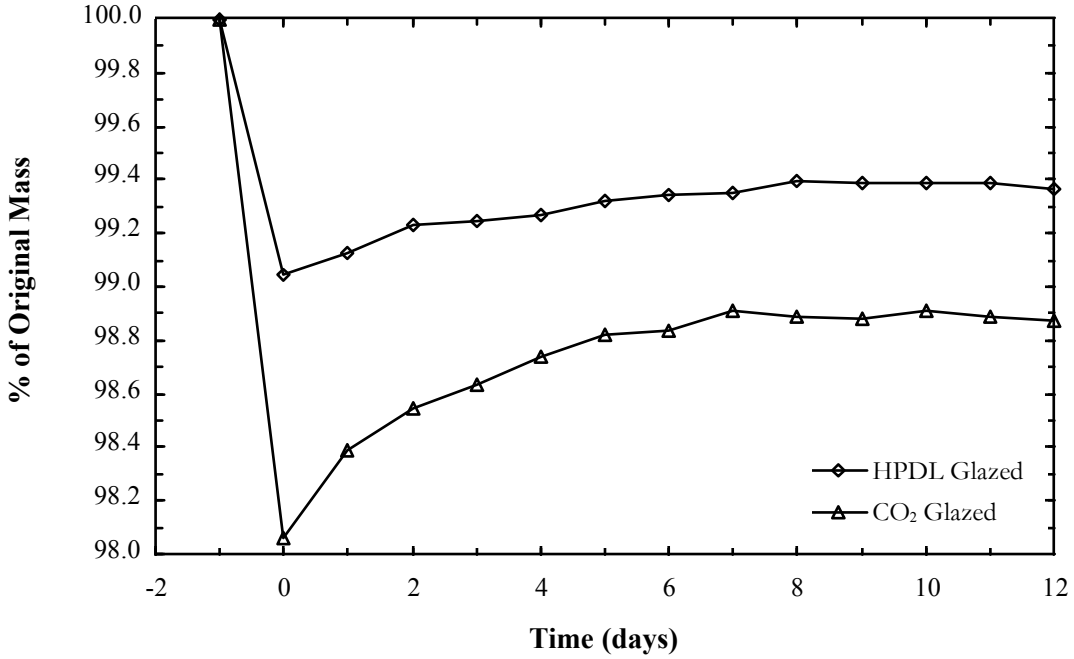
100.0
99.8
99.6
99.4
99.2
99.0
98.8
98.6
98.4
98.2
98.0
% of Original Mass
-2
0
2
4
6
8
10
12
Time (days)
HPDL Glazed
CO2 Glazed

Fig. 4

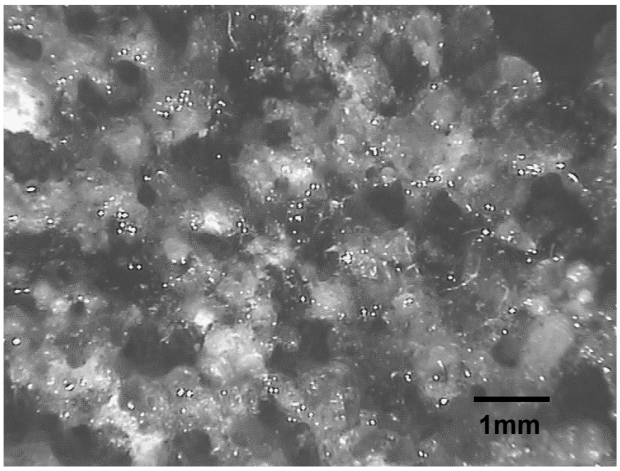

(a)

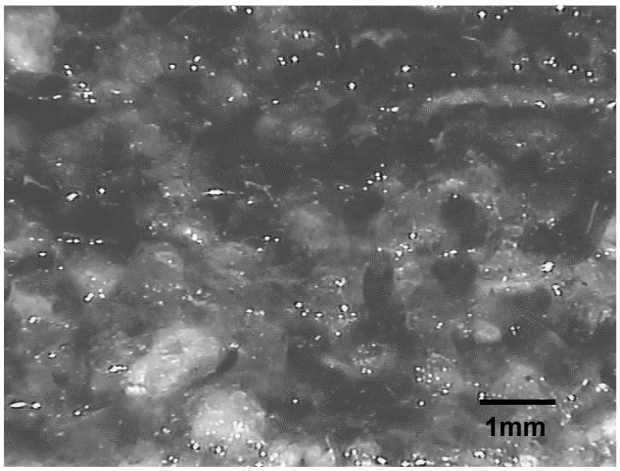

(b)

Fig. 5

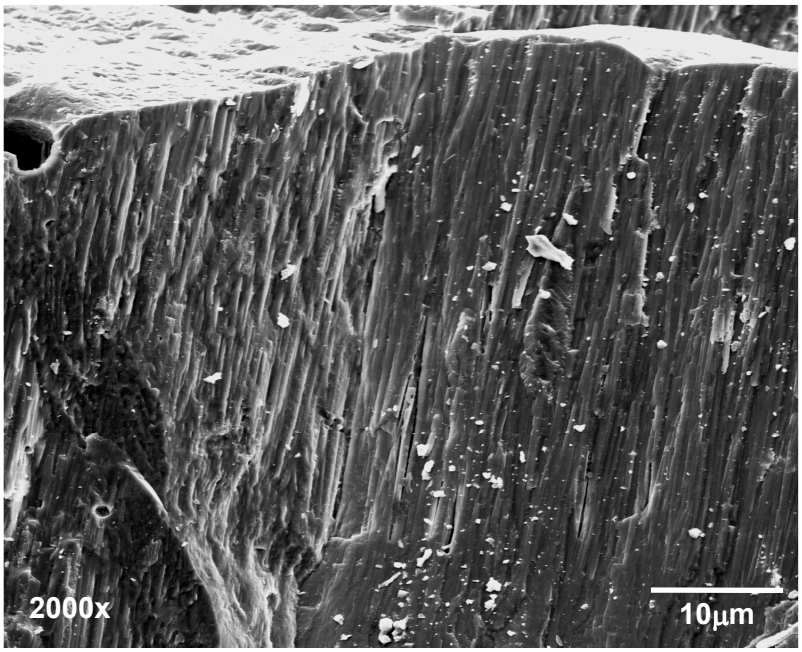

(a)

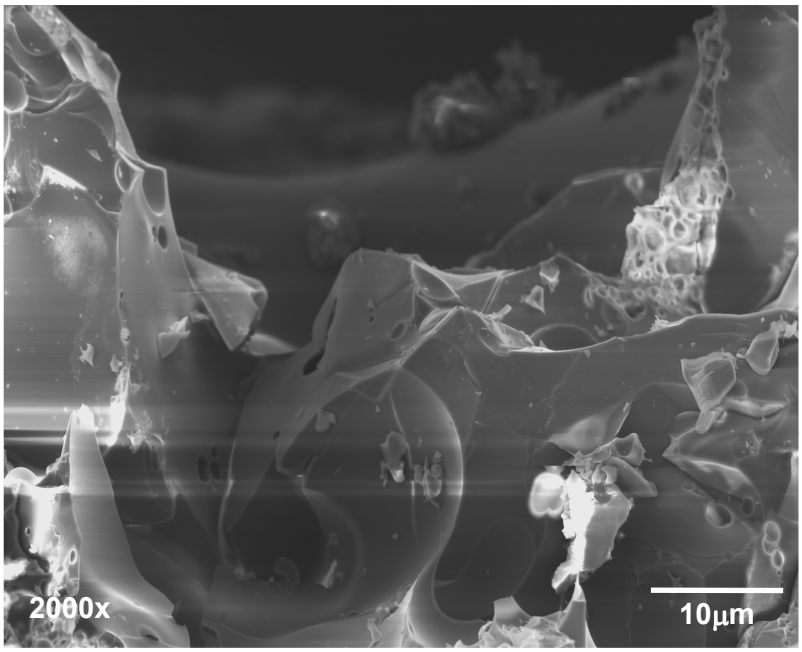

(b)

Fig. 6

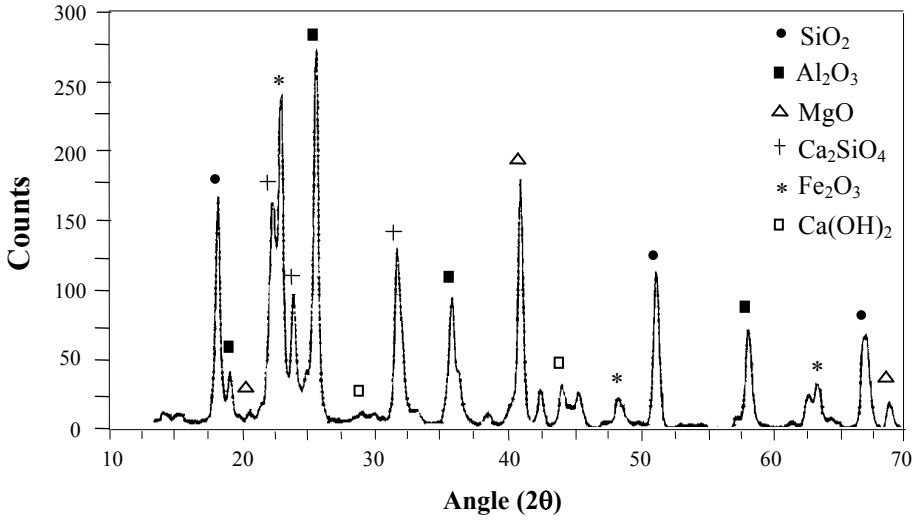
Counts
Angle (2θ)
SiO2
Al2O3
MgO
Ca2SiO4
Fe2O3
Ca(OH)2

(a)

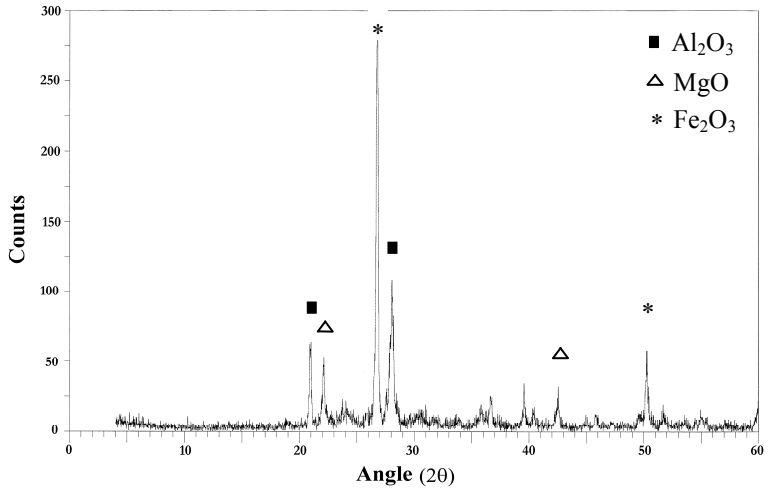
Counts
Angle (2θ)
Al2O3
MgO
Fe2O3

(b)

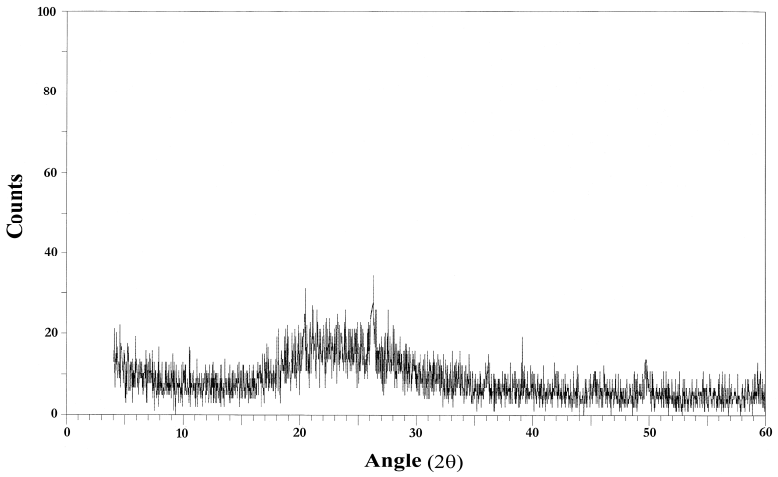

(c)